
Development Characteristics and Influencing Factors of Sweet Spot Reservoirs in Deep and Middle-Layer Tight Sandstone of the Lingshui Formation, Northern Slope of Baodao Depression, Qiongdongnan Basin

Lei Zheng , [Yonggang Zhao](#) * , Turong Wu , Chengfei Luo , Chunyan Zang , [Zhuoyu Yan](#) , Qun Zhang , Xiuzhang Song

Posted Date: 12 January 2026

doi: 10.20944/preprints202601.0848.v1

Keywords: lingshui formation (oligocene); tight sandstone sweet spot reservoirs; controlling factors; pore evolution



Preprints.org is a free multidisciplinary platform providing preprint service that is dedicated to making early versions of research outputs permanently available and citable. Preprints posted at Preprints.org appear in Web of Science, Crossref, Google Scholar, Scilit, Europe PMC.

Copyright: This open access article is published under a [Creative Commons CC BY 4.0 license](#), which permit the free download, distribution, and reuse, provided that the author and preprint are cited in any reuse.

Disclaimer/Publisher's Note: The statements, opinions, and data contained in all publications are solely those of the individual author(s) and contributor(s) and not of MDPI and/or the editor(s). MDPI and/or the editor(s) disclaim responsibility for any injury to people or property resulting from any ideas, methods, instructions, or products referred to in the content.

Article

Development Characteristics and Influencing Factors of Sweet Spot Reservoirs in Deep and Middle-Layer Tight Sandstone of the Lingshui Formation, Northern Slope of Baodao Depression, Qiongdongnan Basin

Zheng Lei^{1,2,3,4}, Zhao Yonggang^{3,4}, Wu Turong^{1,2}, Luo Chengfei^{1,2}, Zang Chunyan¹, Yan Zhuoyu¹, Zhang Qun^{1,2} and Song Xiuzhang¹

¹ CNOOC Central Laboratory, CNOOC EnerTech-Drilling & Production Co., Zhanjiang, 524057, China

² Guangdong Provincial Key Laboratory of Exploration and Development of Complex Oil and Gas Reservoirs in the South China Sea, Zhanjiang, Guangdong 524057, China

³ School of Earth Science and Engineering, Xi'an Shiyou University, Xi'an, 710065, China

⁴ Shanxi Key Laboratory of Petroleum Accumulation Geology, Xi'an Shiyou University, Xi'an, 710065, China

* Correspondence: e-mail: yg_zhao@126.com

Abstract

Deep and middle-layer tight sandstone reservoirs represent an emerging frontier in oil and gas exploration and development. Significant breakthroughs have recently been achieved in the northern deepwater region of the Qiongdongnan Basin, particularly within the Oligocene Lingshui Formation in the Baodao Depression. However, the petrophysical characteristics of these tight sandstone reservoirs and the controlling factors influencing sweet spot development remain poorly understood. This study integrates comprehensive datasets—including thin section petrography, cathodoluminescence, scanning electron microscopy (SEM), X-ray diffraction (XRD), and conventional reservoir property analyses—to systematically investigate the reservoir characteristics and key controls on sweet spot formation in the third member of the Lingshui Formation along the northern slope of the Baodao Depression. A pore evolution model for sweet spot reservoir development is subsequently proposed. The results indicate that: 1) The tight sandstones are predominantly lithic feldspathic quartzarenite, feldspathic quartzarenite, and feldspathic litharenite, with primary pore types including feldspar dissolution pores, moldic pores, and residual intergranular pores. 2) Among these, feldspathic quartzarenite and lithic feldspathic quartzarenite exhibit superior reservoir quality and constitute the main sweet spots; high quartz and feldspar content coupled with low lithic fragment abundance are critical compositional controls on sweet spot formation in deep to middle-depth settings. 3) Grain size demonstrates a positive correlation with reservoir physical properties. Compaction has led to porosity reduction by 22.0%~28.0%, establishing the fundamental basis for reservoir tightness. 4) Dissolution processes play a pivotal role in enhancing reservoir quality. Secondary porosity zones developed at depths of 3800~3950 m and 4100~4400 m due to dissolution significantly improve porosity and permeability. Conversely, during the late stage of mesodiagenesis (Stage B), extensive carbonate cementation contributes to further reservoir compaction. This research provides a theoretical foundation for the evaluation and prediction of sweet spot reservoirs in deepwater tight sandstone systems in the South China Sea, offering guidance for hydrocarbon exploration, field development planning, and the selection of favorable drilling targets. Furthermore, it advances the understanding of the formation mechanisms and evolutionary pathways of different types of sweet spots in deep and middle-layer tight sandstone reservoirs.

Keywords: lingshui formation (oligocene); tight sandstone sweet spot reservoirs; controlling factors; pore evolution

1. Introduction

Deep and middle-layer tight sandstone reservoirs, typically buried between 2000 and 6000 meters, are characterized by significant burial depth, elevated geothermal gradients, high formation pressures, and low matrix permeability. To date, approximately 12×10^{12} m³ of natural gas reserves have been identified in such clastic reservoirs in China, with annual production from deep and middle-layer tight sandstone gas accounting for nearly one-fifth of the nation's total natural gas output. These reservoirs thus constitute a crucial component of China's unconventional hydrocarbon resources, exhibiting substantial exploration and development potential^[1-4]

Globally, deep and middle-depth tight sandstone plays have become increasingly important exploration targets, particularly in mature basins where conventional prospects are diminishing^[5,6]. Recent advancements in geophysical techniques, basin modeling, and unconventional petroleum systems theory have led to significant progress in understanding the genesis, distribution, and evaluation methods of sweet spot reservoirs in tight sandstones. Notably, diagenetic processes have been recognized as key determinants in the development of high-quality reservoir intervals. For example, in the Clair Field of the North Sea, secondary porosity was enhanced through organic acid dissolution—specifically, Permian-sourced organic acids dissolved feldspar grains, generating effective storage space^[7,8]. In the Williston Basin, USA, tight sandstone reservoirs benefit from hydrocarbon charge derived from underlying Bakken shale source rocks, with faulting facilitating efficient vertical migration, illustrating a source-fault-reservoir coupling mechanism^[9-14]. In contrast, in the Santos Basin of Brazil, pervasive carbonate cementation has severely degraded reservoir quality^[15-20]. In China's Ordos Basin, selective dissolution of feldspars has been shown to mitigate compaction effects and preserve primary porosity, whereas rapid burial and intense authigenic mineral precipitation (e.g., quartz overgrowths and clay cements) are primary causes of early reservoir densification^[21-25]. These case studies collectively underscore the dominant control exerted by diagenesis on the heterogeneity and quality of deep and middle-layer tight sandstone reservoirs.

The Qiongdongnan Basin is located in the northern and northwestern parts of the South China Sea. It is a typical Cenozoic faulted rift basin. The deep water areas in its southwestern and northeastern parts are rich in oil and gas resources^[26-28]. Since the exploration of oil and gas in areas such as the Yanan Depression, Ledong-Lingshui Depression, Songnan-Baodao Depression, and Changchang Depression began in the early 1980s, A number of large and medium-sized gas fields and gas-bearing structures have been successively discovered through exploration. Especially from 2013 to 2019, several large and medium-sized deepwater gas fields such as LS17, LS25 and LS22 were successively discovered in the shallow and middle layers of the Ledong-Lingshui depression in the deepwater area. Subsequently, the exploration field of paleogenic oil and gas in the deep and middle layers of the Songnan-Baodao Depression in the eastern part of the basin was gradually expanded. More than 10 Wells were drilled successively. However, due to the small scale of the gas reservoirs, Without obtaining commercial oil and gas reservoirs, it was not until the end of 2020 to 2022 that a major breakthrough in natural gas exploration was achieved for the first time in the third section (tight sandstone) of the Paleogene Oligocene Lingshui Formation on the Northern Slope of the Baodao Depression, based on new research ideas and concepts (conversion of the fault zone) and theoretical and technological innovations. The Baodao 21-1 deepwater and deep (double deep) large gas field was discovered^[29-34]. The Baodao 21-1 gas field is buried relatively deep, and its reservoirs generally feature high temperature, high pressure, poor physical properties, and complex pore structure and genesis^[31]. At present, domestic and foreign researchers' studies on the three sandstone reservoirs of the Lingshui Formation on the Northern Slope of the Baodao Depression mainly focus on converge-source analysis, quantitative characterization of pore structure and sedimentary system, differential evolution of reservoirs, and characteristics of natural gas accumulation, etc^[10 12 18 22], and have made certain progress. However, research on the characteristics of the sweet spot reservoirs of the three sections of tight sandstone in the Lingshui Formation on the Northern Slope of the Baodao

Depression and the mechanism of pore development and evolution is still relatively weak. In view of this, based on previous research and in combination with a large amount of precise, reliable and trustworthy experimental analysis data on petrology, diagenesis and reservoir physical properties obtained in recent years, this paper focuses on conducting in-depth analysis and research on the characteristics of the three sections of tight sandstone reservoirs of the Paleogene Oligocene Lingshui Formation on the Northern Slope of the Baodao Depression, as well as the main controlling factors and pore development and evolution patterns of the sweet zone reservoirs. On this basis, the basic model of pore development and evolution in tight sandstone sweet spot reservoirs is summarized and established, providing important geological basis for the evaluation and prediction of deepwater tight sandstone reservoirs in the northern South China Sea and the selection of oil and gas drilling targets.

2. Regional Geological Overview

The Qiongdongnan Basin is a Cenozoic tensile depression basin in the northern part of the South China Sea, located in the sea area south of Hainan Island and north of the Xisha Islands. It is adjacent to the Pearl River Estuary Basin to the northeast and is controlled by the interaction of regional tectonic forces such as the expansion of the South China Sea, the collision of the Pacific Plate and the Eurasian Plate, and the rotation of the Indochinese Block. From north to south, it is successively divided into primary structural units such as the Northern Depression, the Central Uplift, the Central Depression, and the Southern uplift [29]. Among them, the central depression from west to east can be divided into secondary structural units such as the Ledong Depression, the Lingshui Low Uplift, the Lingshui Depression, the Lingnan Low Uplift, the Beijiao Depression, the Songnan Low Uplift, the Songnan Depression, the Baodao Depression (Songnan-Baodao Depression), and the Changchang Depression. The study area of this study is located in the northeastern part of the Baodao Depression (Figure 1a). The stratigraphic sequence and stratigraphic system filled by Cenozoic sediments, from bottom to top, are the Eocene Lingtou Formation (T100-T80), the Lower Oligocene Yacheng Formation (T80-T70), the Upper Oligocene Lingshui Formation (T70-T60), the Miocene Sanya Formation (T60-T50), Meishan Formation (T50-T40), and Huangliu Formation (T40-T30). The new unified Yinggehai Group (T30-T20) and the new unified - New unified Ledong Group (T20-T10). The basin has undergone three tectonic evolution stages: the early Eocene Early Oligocene depression stage (T100-T70), the Middle Late Oligocene fault-depression transition/post-fracture thermal subsidence stage (T70-T60), and the late Miocene Quaternary depression/post-fracture accelerated thermal subsidence stage (T60 to present) (Figure 1b). The Lingshui Formation, which has the typical characteristics of a lower fault and an upper depression^[31-35], can be further divided from top to bottom into the Lingshui Section 1, Lingshui Section 2 and Lingshui Section 3 during the post-fracture thermal subsidence stage of the late Oligocene fault depression transition/fissure. It belongs to a set of Marine and continental transitional facies and shallow Marine facies deposits. Exploration and research show that during the third sedimentary period of the Late Oligocene, the supply of material sources was abundant, and the main layers were thick gravel sandstone and medium sandstone, with a sand content of over 50%, and sandy sediments were well developed^[36,37]. Under the control and influence of sea level rise and fall and the material supply system, the lower period of the third section of the Lingshui Formation developed a delta sedimentary system and its sandstone reservoirs from the north, while the higher period developed from the northeast. Together with the thick-layered shallow Marine mudstone widely developed in the Lower Miocene (such as the first section of the Sanya Formation, etc.) overlying the third section of the Lingshui Formation, they form a relatively good oil and gas-bearing reservoir cap assemblage type (Figure 1b) The third section of the Paleogene Oligocene Lingshui Formation on the Northern Slope of the Baodao Depression in the northern part of the Qiongdongnan Basin is the study area and stratum of this paper.

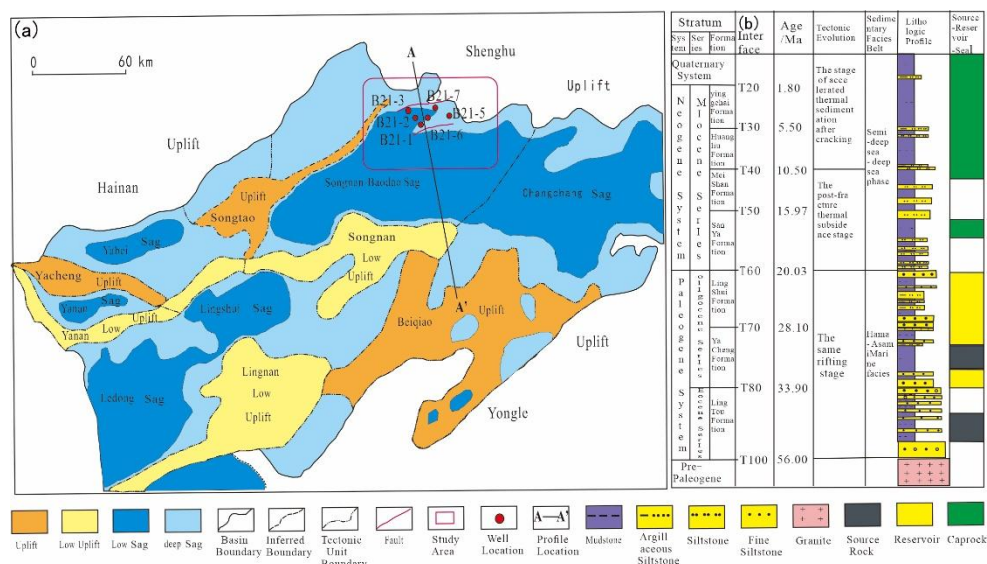


Figure 1. This is a figure. Division of regional tectonic units in the Qiongdongnan Basin and the tectonic position of the study area (a) and the comprehensive columnar section of the Cenozoic stratigraphic system (b)

3. Materials and Methods

A total of 268 sidewall and core samples were collected for this study. Three analytical methods were employed:

1. Petrographic Thin Section Analysis: Rocks were impregnated with blue epoxy resin and prepared into standard thin sections of 0.03 mm thickness. After staining with a mixed Alizarin Red-S and potassium ferricyanide dye, mineral and pore types were identified using a Zeiss microscope (ZEISS Imager A2m). Their contents were then quantified using the Gazzi-Dickinson method.

2. Scanning Electron Microscopy (SEM) Analysis: Fresh, flat surfaces of the samples were selected and coated in a vacuum environment. The mineral structures were analyzed using a field emission scanning electron microscope (FEI Quanta 650 FEG) equipped with an energy-dispersive spectrometer (Bruker XFlash630 EDS). The operating parameters were as follows: voltage of 20 kV, filament current of 2400 mA, beam diameter of 4 nm, and resolution ≤ 2.5 nm.

3. Cathodoluminescence (CL) Analysis: Rocks were impregnated and consolidated with α -cyanoacrylate or epoxy resin, and prepared into thin sections of 0.04 mm thickness. After staining, the luminescence characteristics of the minerals were observed using a Leica microscope (DM4500P) within the vacuum chamber of a cathodoluminescence device (CLF-2). The operating parameters were: voltage of 12.5 kV, current of 0.256 mA, and vacuum level of 0.004 mbar.

4. Results

4.1. Petrological Characteristics of Tight Sandstone Reservoirs

A comprehensive analysis of 268 wellbore cores and rock cores from 6 Wells in the study area, including thin section identification, cathode luminescence and scanning electron microscopy, shows that the rock types of the third section of the tight sandstone reservoir of the Upper Oligocene Lingshui Formation in the Baodao 21-1 gas field in the study area. The main types are feldspar quartz sandstone, feldspar quartz sandstone and feldspar feldspar quartz sandstone (in accordance with the enterprise standard Q/HXJ1039-93 "Identification of Sandstone Flakes"). Among them, the framework of the rock debris particles is basically composed of quartz, feldspar and rock debris. The feldspar component is weathered to medium-deep, and the fillers are mainly argillaceous, carbonate and clay minerals. The overall rock sorting is moderate, mainly featuring secondary ridges and secondary circles (Figures 2 and 3).

Among them, the quartz content in feldspar quartz sandstone ranges from 40.0% to 66.5%, with an average of 55.6%. The feldspar mainly consists of potassium feldspar and a small amount of plagioclase, with an feldspar content of 8.0%~18.5% and an average of 12.8%. The cuttings mainly include mica quartz schiss, porphyry and a small amount of granite, with a cuttings content of 7.0%~12.0% and an average of 9.2%. In addition, it contains a small amount of mud, with an average value of 1.6%. The content of calcite and iron calcite in carbonate cements ranges from 0%~33%, with an average of 2.4%, and the content of dolomite and iron dolomite ranges from 0%~13%, with an average of 2.4%. The content of siderite ranged from 0%~25%, with an average of 1.3%. The siliceous cementation content ranged from 0%~3.0%, with an average value of 0.7%. Among the self-generated cements, the content of clay minerals (kaolinite, chlorite, and water mica) is relatively low, ranging from 0%~1.0%, with an average of 0.3%.

The quartz content in feldspar quartz sandstone ranges from 47.0%~70.0%, with an average of 59.3%. The feldspar content ranges from 7.5%~20.5%, with an average of 14.4%, and the cuttings content is 3.5%~8.0%, with an average of 6.3%. A small amount of mud, with an average value of 2.9%. The contents of calcite and iron calcite in carbonate cements ranged from 0.0%~25.0%, with an average of 2.1%, and the contents of dolomite and iron dolomite ranged from 0.0%~26.0%, with an average of 2.4%. The content of siderite ranged from 0.0%~3.0%, with an average of 0.7%. The siliceous cementation content ranged from 0.0%~1.5%, with an average of 0.8%. Among the self-generated cements, the content of clay minerals (kaolinite, chlorite, and water mica) is relatively low, ranging from 0.0%~0.5%, with an average of 0.1%.

The quartz content in feldspar quartzite sandstone ranges from 46.0%~67.0%, with an average of 56.6%. The feldspar content ranged from 8.5%~12.0%, with an average of 9.3%, and the cuttings content ranged from 9.0%~13.0%, with an average of 10.1%. The mud is underdeveloped. The contents of calcite and iron calcite in carbonate cements ranged from 2.0%~25.0%, with an average of 7.5%, and the contents of dolomite and iron dolomite ranged from 0.0 %~7.0%, with an average of 1.0%. The content of siderite is 0.0 %~0.5%, with an average of 0.2%. The siliceous cementation content ranged from 0.0 %~1.5%, with an average of 0.5%. Among the self-generated cements, the content of clay minerals (kaolinite, chlorite, and water mica) is relatively low, ranging from 0.0 %~0.5%, with an average of 0.2% (Figure 4).

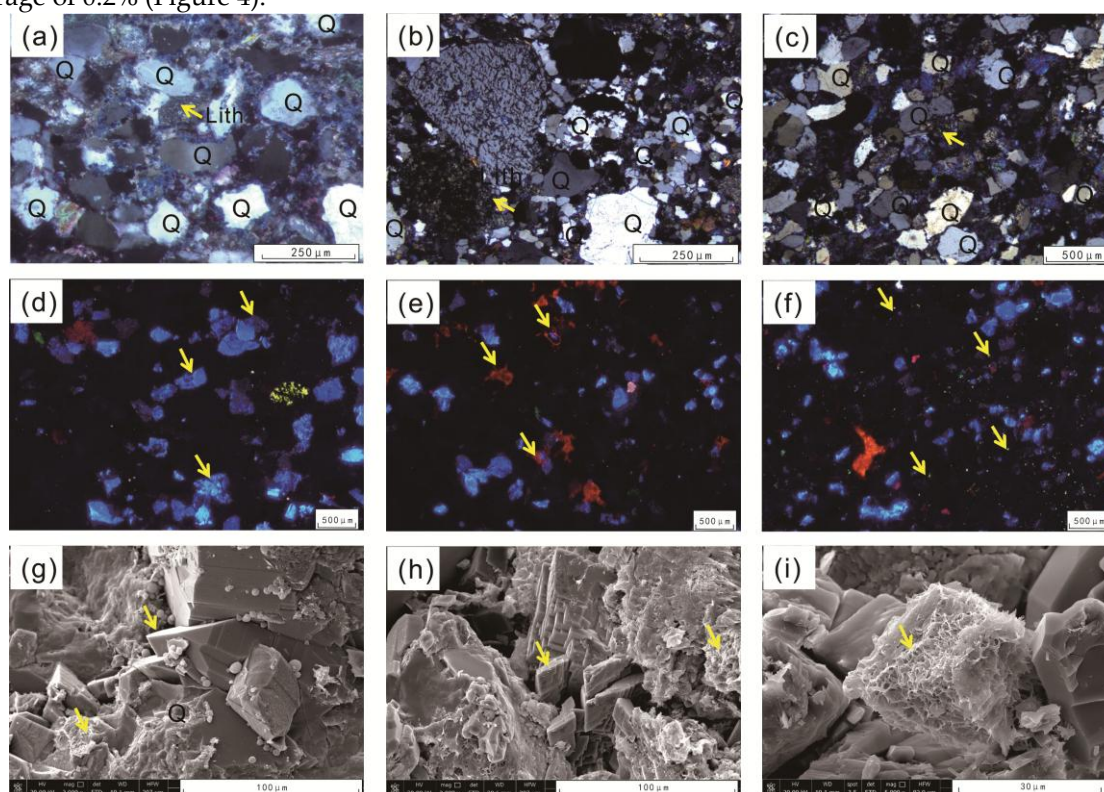


Figure 2. This is a figure. is a microscopic photograph of the petrological characteristics of the tight sandstone reservoir in the third section of the Jianxin Tongling in the study area.

(a) Well B21-1, 4172.0 m, Section 3 of Lingshui Formation, rock cuttings feldspar quartz extremely fine - fine sandstone; (b) Well B21-2d, 4300.56m, Section 3 of Lingshui Formation, feldspar quartz fine - extremely coarse sandstone; (c) Well B21-2d, 4301.79m, Section 3 of Lingshui Formation, feldspar quartzite fine to medium sandstone; (d) Well B21-1, 4121m, Section 3 of Lingshui Formation, potassium feldspar emits a blue light;

(e) Well B21-5, 3826.9m, Section 3 of the Lingshui Formation, developed two stages of calcite cementation. In the first stage, the calcite was arranged to form feldspar particles or filled between the particles, emitting an orange-red light. In the second stage, it emitted an orange-yellow light and filled around the cementation of the first stage in a ring shape; (f) Well B21-6d, 4416.0m, Section 3 of Lingshui Formation, plagioclase dark blue light, grass green light (mudization); (g) Well B21-2d, 4494.0m, Section 3 of Lingshui Formation, the pores are filled with autohedral quartz, and Immon mixed layers develop between the intergranular pores of quartz; (h) Well B21-3d, 4223.6m, Section 3 of Lingshui Formation, the pores are filled with clay minerals such as autoform dolomite, quartz and Imon mixed layers; (i) Well B21-6d, 4,397.0 m, Section 3 of the Lingshui Formation, the intergranular pores are filled with filamentous illite.

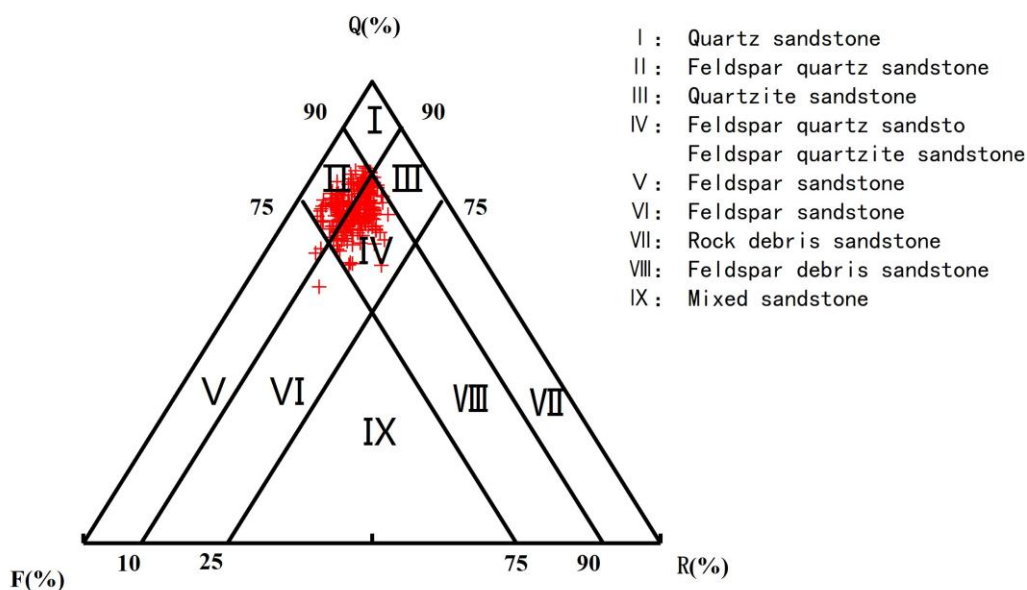


Figure 3. This is a figure. shows the triangular diagram of rock composition in the tight sandstone reservoir of the third section of the Upper Oligocene Ridge in the study area.

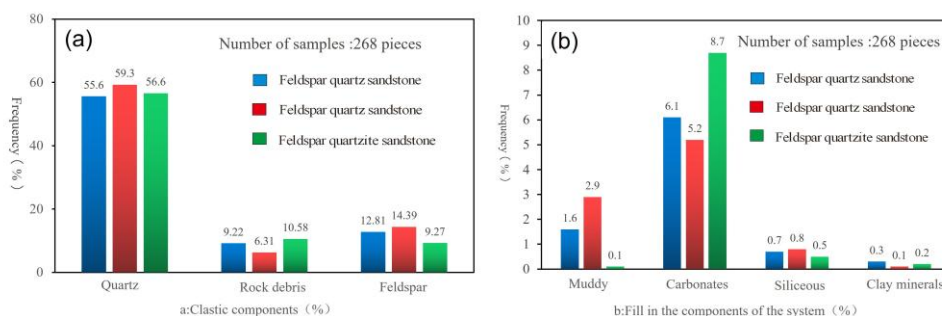


Figure 4. This is a figure. shows the statistical histogram of rock composition in the tight sandstone reservoir of the third section of the Upper Jiaoxin Tongling in the study area.

4.2. Pore Development Characteristics of Tight Sandstone Reservoirs

Through the observation of the thin cast sections of the third stage of the Lingshui Formation, it was found that the pore types of the reservoirs in the third stage of the Lingshui Formation in the study area mainly include feldspar dissolution pores, mold pores, remaining intergranular pores, intergranular dissolution pores and intra-granular dissolution pores, totaling five categories. Among them, the remaining intergranular pores, feldspar dissolution pores and mold pores are the main types of reservoir Spaces in the three sections of the Lingshui Formation in this area. The porosity of intergranular pores was approximately 0.0%~7.0%, with an average of 1.31%. The porosity of feldspar dissolved pores is approximately 0.0%~9.0%, with an average of 3.90%. The porosity of the mold holes is approximately 0.0%~11.0%, with an average of 3.57%. The porosity of the intergranular dissolution pores in the secondary pores is approximately 0.0%~2.0%, with an average of 0.44%, and the porosity of the intra-granular dissolution pores is approximately 0.0%~7.0%, with an average of 0.59%. The intergranular and intra-granular dissolution pores have a relatively small impact on the pore reservoir performance of the reservoir (Figure 5).

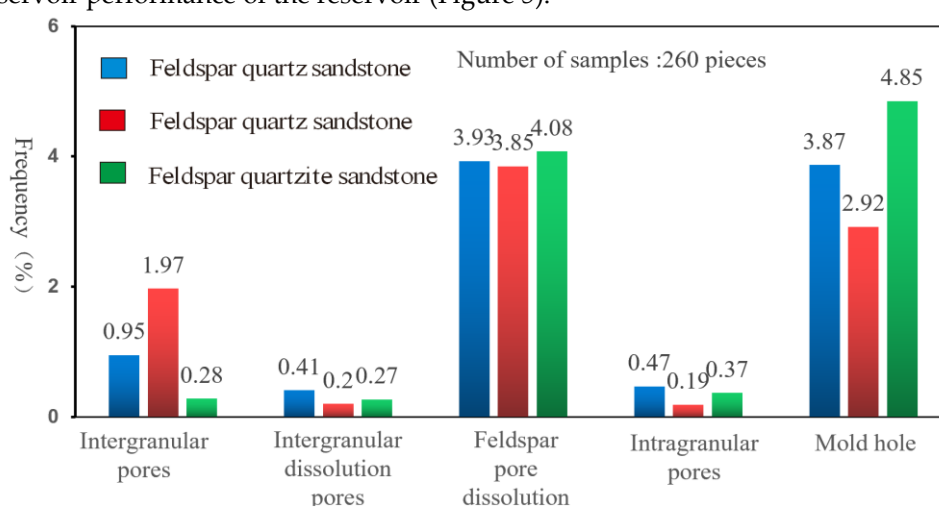


Figure 5. This is a figure. shows the distribution histogram of pore types in the tight sandstone reservoirs of the third section of the Upper Oligocene Ridge in the study area.

Overall, the intergranular pores of the feldspar quartz sandstone reservoir are regular in shape, with straight edges, presenting relatively regular triangles, polygons, etc. [Figure 6(a)], and there are no obvious traces of dissolution and modification. Secondary pores are mainly formed by the selective dissolution of acidic unstable minerals such as feldspar and rock debris, resulting in mold holes and feldspar dissolution holes. The shape of feldspar dissolution holes is irregular, often presenting as banded, honeycomb-like, plate-like, serrated or harbin-like dissolution forms [Figure 6(b)], and the connectivity between the pores is poor. It was also observed that the secondary enlargement of quartz altered the size and shape of intergranular pores [Figure 6(c)]. The analysis of casting thin sections and images shows that the overall porosity of the feldspar quartz sandstone reservoir is approximately 9.63%. Among them, the porosity of feldspar dissolution holes mainly ranges from 0.0%~9.0%, with an average of 3.93%, and the porosity of mold holes mainly ranges from 0.0%~9.0%, with an average of 3.87%. The porosity of intergranular pores mainly ranged from 0.0%~7.5%, with an average of 0.95%. The second type is the intergranular dissolution pores and the intra-granular dissolution pores. The proportions of porosity were 0.41% and 0.47% respectively. Among them, intergranular pores accounted for approximately 9.87% of the total porosity, feldspar dissolution pores accounted for approximately 40.81%, and mold pores accounted for approximately 40.19%. The statistical results of image analysis show that the pore radius of the feldspar quartz sandstone is between 5.95 and 117.92 μm , with an average value of 42.41 μm .

The feldspar quartz sandstone reservoir has a high content of rigid particles. The content of plastic particles is relatively low; It has a strong resistance to compaction, with well-developed

intergranular pores remaining, and relatively low feldspar dissolution pores and mold pores. The overall porosity is approximately 9.13%. Among them, the porosity of feldspar dissolution holes mainly ranges from 0.0%~4.0%, with an average of 3.85%, the porosity of mold holes mainly ranges from 0.0%~10.0%, with an average of 2.92%, and the porosity of intergranular holes mainly ranges from 0.0%~7.5%, with an average of 1.97%. The second type is the intergranular dissolution pores and the intra-granular dissolution pores. The proportions of porosity were 0.20% and 0.19% respectively. It was observed that the rock debris particles were completely eroded, leaving only the particle Outlines and forming mold holes [Figure 6(d)]. Among them, intergranular pores accounted for approximately 21.58% of the total porosity, feldspar dissolution pores accounted for approximately 42.17%, and mold pores accounted for approximately 31.98%. The statistical results of image analysis show that the pore size of feldspar quartz sandstone reservoirs is generally between 0.95 and 118.01 μm , with an average value of 38.34 μm .

The average porosity of feldspar quartzite sandstone reservoirs is approximately 9.85%. Among them, the porosity of feldspar dissolution holes mainly ranges from 1.0%~7.0%, with an average of 0.28%, the porosity of mold holes mainly ranges from 1.5%~11.00%, with an average of 4.85%, and the porosity of intergranular holes mainly ranges from 0.0% ~0.3%. The average value was 0.28%, followed by intergranular dissolution pores and intra-granular dissolution pores. The proportions of face rates were 0.27% and 0.37% respectively. Feldspar shavings quartz sandstone is mainly characterized by intense plastic shavings deformation and strong dissolution, with relatively poor development of intergranular pores, intergranular dissolution pores and intra-granular dissolution pores [Figure 6(e)]. Due to the strong corrosive effect, the mold holes are relatively well developed [Figure 6(f)]. Among them, intergranular pores accounted for approximately 2.84% of the total porosity, feldspar dissolution pores accounted for approximately 41.42%, and mold pores accounted for approximately 49.24%. The statistical results of image analysis show that the pore size of sandstone reservoirs is generally 3.59~100.37 μm , with an average value of 42.30 μm .

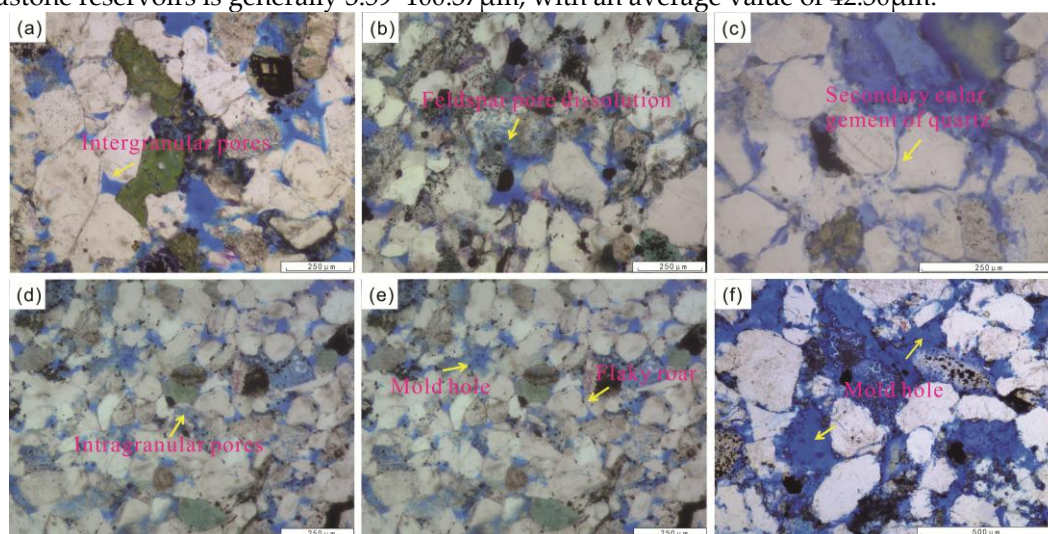


Figure 6. This is a figure. shows the basic microscopic characteristics of pore types in the tight sandstone reservoirs of the third section of the Upper Oligocene Ridge in the study area.

(a) Well B21-5,3826.9m, Section 3 of Lingshui Formation, cuttings feldspar quartz fine to medium sandstone; (b) Well B21-1, 4,147.0 m, Section 3 of Lingshui Formation, cuttings feldspar quartz medium-fine sandstone;(c) Well B21-2d, 4263.5m, Section 3 of Lingshui Formation, cuttings feldspar quartz medium-fine sandstone; (d) Well B21-3d,4221.3m, Section 3 of Lingshui Formation, feldspar quartz extremely fine - fine sandstone; (e) Well B21-1, 4130.0m, Section 3 of Lingshui Formation, feldspar cuttings quartz extremely fine - fine sandstone; (f)Well B21-2d,4307.82m, Section 3 of Lingshui Formation, cuttings feldspar quartz fine to medium sandstone

4.3. Reservoir Physical Property Characteristics of Tight Sandstone Reservoirs

A comprehensive evaluation of the three tight sandstone reservoirs of the Lingshui Formation was conducted based on conventional physical property data. Among the reservoir physical property parameters of the three reservoirs of the Lingshui Formation, the average permeability was $3.85 \times 10^{-3} \mu\text{m}^2$, and the maximum porosity was 11.16%. The overall physical properties of the reservoirs were mainly characterized by low porosity and low permeability (according to DZ/T0217-2005). However, there are still relatively obvious differences among feldspar quartz sandstone, feldspar quartz sandstone and feldspar feldspar quartz sandstone. The porosity of the feldspar quartz sandstone reservoir ranges from 4.70%~16.30%, with an average value of 11.48%. Permeability between $(0.05\sim 68.4) \times 10^{-3} \mu\text{m}^2$, with a mean of $1.78 \times 10^{-3} \mu\text{m}^2$ (figure 7 (a), figure 7 (b)), for the low hole - low permeability reservoir. The porosity of feldspar quartz sandstone ranges from 2.86%~18.20%, with an average of 10.92%. Permeability between $(0.050 \sim 268.0) \times 10^{-3} \mu\text{m}^2$, with a mean of $6.73 \times 10^{-3} \mu\text{m}^2$ (figure 7 (c), figure 7 (d)), for the low hole-low permeability reservoir. The porosity of feldspar quartzite sandstone ranges from 5.54%~13.30%, with an average of 10.21%. The permeability ranges from $(0.050 \text{ to } 0.466) \times 10^{-3} \mu\text{m}^2$, with an average of $0.26 \times 10^{-3} \mu\text{m}^2$ [Figure 7(e), Figure 7(f)], and it is a low-porosity-ultra-low-permeability reservoir. The statistical results show that the reservoir physical properties of feldspar quartz sandstone and cuttings feldspar quartz sandstone are relatively good, followed by feldspar cuttings quartz sandstone.

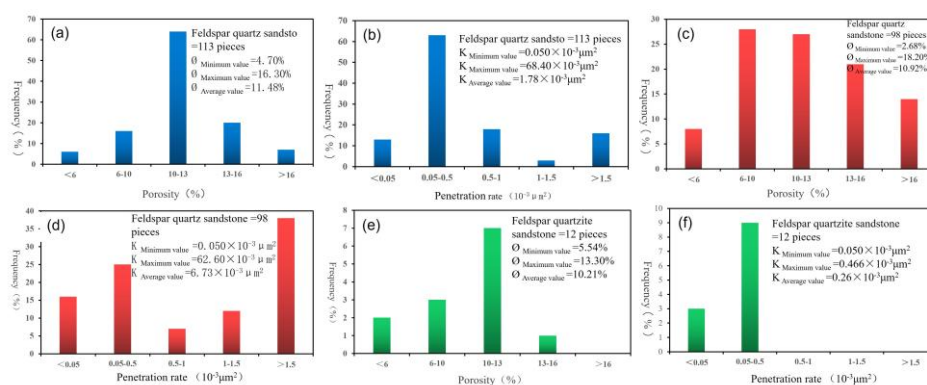


Figure 7. This is a figure. shows the distribution histogram of reservoir physical properties in the tight sandstone reservoir of the third section of the Lower Oligocene Ridge in the study area.

5. Discussion

During the process of sedimentary burial and diagenesis, the original pores will undergo significant changes under the effects of diagenetic compaction, cementation and dissolution. Among them, diagenetic compaction and cementation are the most significant destructive diagenetic processes, which greatly reduce the porosity and permeability of rocks. Dissolution, on the other hand, is the most important constructive diagenetic process, which leads to the generation of a large number of secondary pores in reservoir rocks and effectively increases the reservoir space^[38-40]. Therefore, the degree of reservoir pore development is mainly controlled by the constraints and influences of diagenesis, the source supply system, the sedimentary environment and sedimentary equivalence factors.

5.1. The Influence of Different Terrigenous Clastic Components on Reservoir Physical Properties

The sedimentary environment and sedimentary facies control the type of reservoir sand body and are important factors determining the pore seepage characteristics of the reservoir. The hydrodynamic conditions vary in different sedimentary environments, which leads to significant differences in the composition, grain size, sorting, cementation type and pore filling mode of clastic sedimentary rocks. Therefore, the sedimentary environment and sedimentary processes have a

significant impact on the reservoir physical properties of the formed reservoirs. The general sedimentary processes mainly include transportation, rounding, sorting, and sedimentation. The internal structure, bedding structure, morphology, lateral continuity, and longitudinal continuity of the formed reservoir sand bodies all have varying degrees of differences. It can be seen that sedimentary processes are the re-shaping and recombination of the original diagenetic materials by sedimentary dynamic forces, and to a certain extent, they affect the reservoir physical properties. The rock types in the third section of the Lingshui Formation are mainly feldspar quartz sandstone, cuttings feldspar quartz sandstone and feldspar cuttings quartz sandstone. The main mineral components are quartz, feldspar and rock debris. By statistically analyzing the relationship between quartz, feldspar and cuttings of the three stages of the Lingshui Formation and the reservoir physical properties of the reservoir (Figure 8); It can be seen that quartz, feldspar and cuttings have little influence on the porosity of the reservoir. Quartz and feldspar have a relatively weak positive correlation with permeability. Cuttings have a strong negative correlation with permeability. This paper conducts a comprehensive analysis of the three rock skeletons of the Lingshui Formation and holds that a high content of quartz and feldspar and a relatively low content of cuttings are one of the main controlling conditions for the formation of sweet spot reservoirs in the middle and deep layers of tight sandstone.

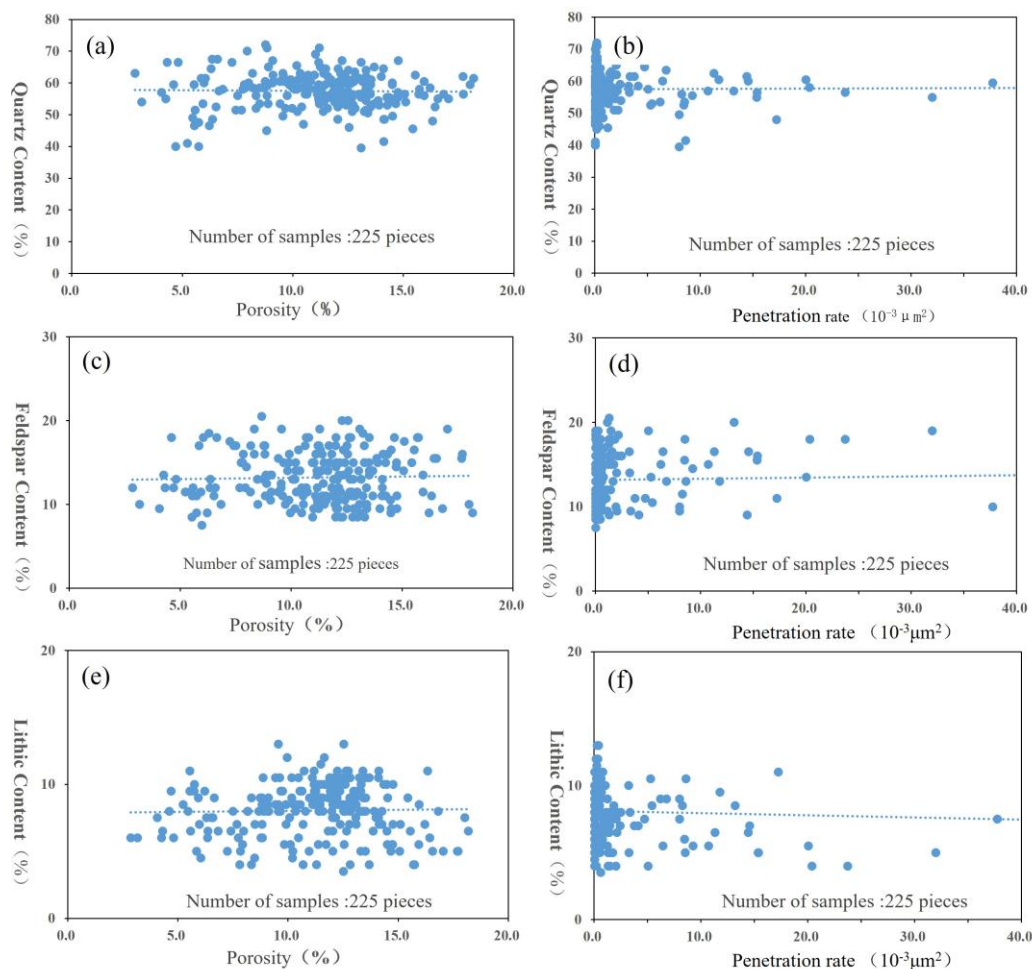


Figure 8. This is a figure. shows the relationship between different terrigenous clasts and reservoirs in the dense sandstone reservoirs of the third section of the Upper Oligocene Ridge in the study area.

5.2. The Influence of Grain Size and Sortability on the Reservoir Physical Properties of Tight Sandstone Reservoirs

The Lingshui Formation in the study area has developed three large delta sandstone reservoirs. The reservoir sandstones mainly include fine-grained to coarse sandstone, medium-coarse sandstone, fine-grained to medium sandstone, medium-fine sandstone and fine-grained to extremely fine sandstone, etc. The statistical results show that the porosity of fine-coarse sandstone and medium-coarse sandstone ranges from 4.26%~15.90%, with an average value of 11.04%. Permeability between $(0.101\sim62.60)\times 10^{-3}\mu\text{m}^2$, with a mean of $4.94\times 10^{-3}\mu\text{m}^2$ [figure 9 (a), figure 9 (b)]. The porosity of coarse-medium sandstone and fine-medium sandstone ranges from 4.31%~17.7%, with an average of 11.78%. Permeability between $(0.050\sim 268)\times 10^{-3}\mu\text{m}^2$, with a mean of $12.5\times 10^{-3}\mu\text{m}^2$ [figure 9 (c), figure 9 (d)]. The porosity of medium-fine sandstone and extremely fine sandstone reservoirs ranges from 5.54%~16.30%, with an average of 11.15%. Permeability between $(0.05\sim 14.4)\times 10^{-3}\mu\text{m}^2$, with a mean of $1.14\times 10^{-3}\mu\text{m}^2$ [figure 9 (e), figure 9 (f)]. The porosity of silty extremely fine sandstone and fine-to-extremely fine sandstone reservoirs ranges from 3.17%~12.80%, with an average value of 8.62%. Permeability between $(0.05\sim 3.76)\times 10^{-3}\mu\text{m}^2$, with a mean of $0.33\times 10^{-3}\mu\text{m}^2$ [figure 9 (g), figure 9 (h)]. From the relationship diagram of the three-stage grain size and porosity of the Lingshui Formation, it can be seen that the coarse and medium-grained sandstones representing strong hydrodynamic conditions and the fine and extremely fine sandstones have higher original physical properties under the same burial depth conditions, and their compressive resistance during the burial process is also relatively stronger. Therefore, the control effect of clastic particle size on physical properties is particularly obvious (Figure 9). Overall, the particle size of sandstone samples has a good positive correlation with reservoir physical properties. The larger the clastic particle size, the higher the porosity and permeability values tend to be. Due to the mechanical separation effect during the long-distance transportation of clastic materials, the larger the particle size and the better the separation of the sandstone, the lower the content of plastic rock debris is often. Secondly, the finer the particle size and the poorer the separation of the sandstone, the higher the content of plastic rock debris. On the other hand, the better the sample's separability, the relatively lower the argillaceous content. Fewer argillaceous impurities in the pores are conducive to the preservation of the pores between the primary grains. Thin slice observations show that the content of argillaceous impurity groups in high-quality reservoir sandstones is basically less than 0.5%, while the physical properties of marginal sandstone samples with higher contents of argillaceous bands and argillaceous masses are relatively poor. It is further proved that grain size and sortability are important factors influencing the formation of tight sandstone sweet spot reservoirs.

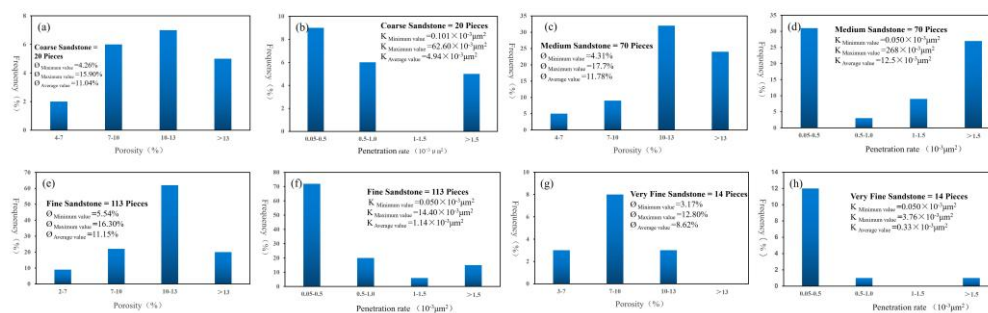


Figure 9. This is a figure. shows the relationship between reservoir physical properties and grain size of the tight sandstone reservoir in the third section of Ling in the study area

5.3. The Control Effect of Compaction on Primary Pores

Compaction is the most significant destructive diagenetic process that controls and affects the porosity and permeability of tight sandstone reservoirs. After the third section of the Lingshui Formation was buried, as the overlying strata (Sanya Formation, Meishan Formation, Huangliu Formation) and other sediments continuously thickened, the formation pressure gradually increased. The sediments began to drain water, the porosity decreased, the volume shrank, and gradually transformed towards densification. As the burial depth increases, the static pressure of the stratum becomes greater and greater, and the compaction effect becomes more intense. After rock consolidation, the main manifestation is the continuous increase in the tightness of contact between particles and interstitial substances. In addition to being affected by the external factor of burial depth, the

characteristics of the sediment itself often have a significant impact on the intensity of mechanical compaction. Meanwhile, the mineral composition and content of the interstitial debris also play a certain controlling role in mechanical compaction. Due to the medium sorting coefficient of the tight sandstone in the study area, the average original porosity was calculated at OP=40%. The total apparent porosity, calcite, iron calcite, dolomite, iron dolomite, siderite, pyrite and aquite of the three sections of the Lingshui Formation were statistically analyzed (Table 1). The average COPL (original porosity) of the compaction loss of the three sections of the Lingshui Formation's tight sandstone was calculated to be 24%, and its CPI (compaction strength coefficient) was 60% (Table 2), which belongs to strong compaction. Due to the influence of strong compaction, the clastic particles in tight sandstone mainly come into contact with lines and concave-convex lines, with a small amount of point-line contact. The clastic particles are mainly supported by the particles, and the overall sorting is moderate. Some schist chips, phyllite chips, mica chips, altered volcanic rock chips, and argillaceous layers are often compressed and deformed into a "curved arch shape". Some altered particles, such as kaolinized feldspar particles, are often squeezed into the intergranular spaces to form false impurity groups. It can be intuitively reflected from (Table 1) that, apart from the local dense cementation, the sandstone compaction is the most severely affected. The burial compaction leads to a loss of 22.0%~28.0% of the sandstone porosity, with an average of over 24.0%, resulting in a rapid reduction of the primary pores in the three sections of the Lingshui Formation in the study area and forming a background of dense sandstone reservoirs.

Table 1. This is a table. shows the statistics of intergranular volume of tight sandstone reservoirs in the third section of the Upper Oligocene Ridge in the study area.

Well	depth /m	porosity	Content (%)						
			Calcite	Ankerite	Dolomite	Ankerite	Siderite	Pyrite	Aquamarine
B21-1	4112.5-5002	5.6	1.1	2.5	1.1	2.5	0.2	0.9	2.6
B21-2d	4144.6-4628	9.8	0.3	2.6	0.4	1.6	0.8	0.3	1.8
B21-3d	4198-4434	9.1	0.7	1.1	1	0.6	0.6	1	3.1
B21-5	3673.4-4251	6.8	0	2.9	0.2	1.7	1.1	0.2	1.9
B21-6d	4049.6-4430	12.2	0.1	0.9	0.3	2.5	0.2	0.6	1.1
B21-7d	4300-4780	4.5	0	2.5	0.4	1.8	0.4	0.2	2.1

Table 2. This is a table. shows the statistical data of the compaction intensity of the tight sandstone reservoirs in the third section of the Upper Oligocene Ridge in the study area.

Well	depth /m	IGV	Content (%)				Average	CPI
			CEM	OP	COPL			
B21-1	4112.5-5002	16.5	10.9	40	24	24	60	
B21-2d	4144.6-4628	17.6	9.6	40	22			
B21-3d	4198-4434	17.2	8.1	40	23			
B21-5	3673.4-4251	14.8	8	40	25			
B21-6d	4049.6-4430	17.9	5.7	40	22			
B21-7d	4300-4780	11.9	7.4	40	28			

Note: IGV (Intergranular Volume) CEM (cementing material + authigenic minerals) OP (Original Porosity); COPL(Original porosity lost due to compaction) CPI (Compaction Strength Coefficient)

5.4. The Influence of Cementation on the Physical Properties of Tight Sandstone Reservoirs

Cementation is one of the important reasons for reducing primary pores and roaring channels, and it is also a major destructive diagenetic process and a key factor controlling the quality of reservoir porosity and permeability. Through the analysis of the study area, it was found that the

cementation mainly includes carbonate cementation, siliceous cementation and clay mineral cementation, etc. The statistical results show that the content of carbonate cementation is generally 0.5%~30.5%, with an average of 6.28%. Carbonate cementation is mainly pore cementation, unevenly filling the pore edges and metasomating the rocks. Occasionally, early calcite shows intercalation cementation. The higher the content of cementing material, the worse the physical properties of the reservoir. The formation of intercalated cemented calcite is mainly related to the relatively high concentration of calcium ions and carbonate ions in the bottom water, and it mainly develops in the early rock formation B stage. Porous cemented iron calcite and iron dolomite mainly develop in the middle diagenetic stage B. When the diagenetic environment gradually changes to an alkaline environment, iron calcite and iron dolomite re-precipitate and fill the residual intergranular pores and erosion pores. Siliceous cementation is mainly secondary enlarged and relatively self-shaped microcrystalline quartz, mainly porous cementation, with a content generally ranging from 0.0%~1.5%, and an average of 0.52%. Clay minerals are mainly produced at the edges or inside the particles, with a relatively low content of 0.0%~2.0% and an average value of 0.15%. It has a relatively small impact on physical properties. Kaolinite is generally in the form of vermicular or pseudo-book page aggregates, occurring in the form of pore filling or metasomatism with other minerals. Under electron microscopy, illite mainly appears in filamentous, band-like, irregular flaky, curved and thread-like forms, covering the surface of particles or filling pores and crevices [Figure 2(i)].

This paper's comprehensive analysis reveals that cementation has a significant impact on the reservoir physical properties. The remaining intergranular pores are further depleted after compaction. Therefore, cementation is the secondary cause of the reduction in sandstone physical properties. The results of the thin sheet point analysis show that for the three sections of sandstone in the Lingshui Formation, calculated at an average original porosity OP of 40% (Table 1), cementation leads to a porosity loss of 5.7%~10.9%, with an average of 8.28% (Figure 10). The porosity lost due to burial compaction far exceeds that lost due to cementation. Therefore, it is well proved that compaction is the most important factor causing the reduction of porosity in the study area.

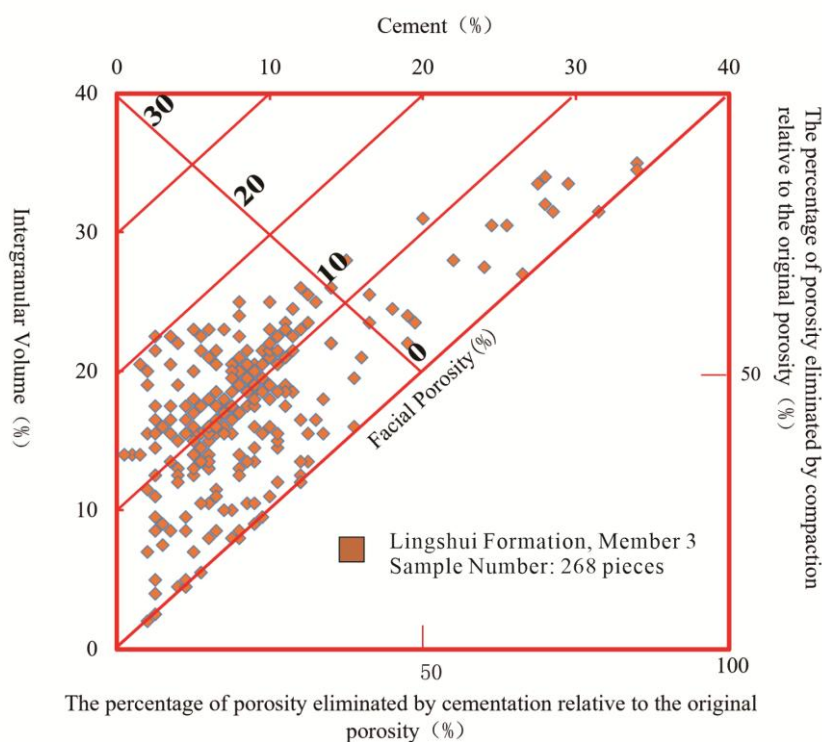


Figure 10. This is a figure. shows the types of cementation in the dense sandstone reservoirs of the third section of the Upper Oligocene Ridge in the study area

5.5. Dissolution is a Key Factor in the Formation of Sweet Spot Reservoirs of Middle and Deep Tight Sandstone

Rock thin sections and scanning electron microscopy observations indicate that the degree of sandstone erosion in the three sections of the Lingshui Formation in the study area is relatively intense [Figure 6(f)]. Three sets of source rocks, namely the Eocene lacustrine mudstone, the Lower Oligocene coal-bearing and Marine mudstone, and the upper Oligocene - Miocene Marine mudstone, have developed in the Qiongdongnan Basin. These have been confirmed in the exploration practice. The coastal plain coal-bearing strata and Marine mudstone of the Yacheng Formation of the Lower Holocene are the main source rocks^[29-35]. Through detailed structural evolution profile analysis (Figure 12), it can be clearly seen that the Northern Slope zone of the Baodao Depression in the study area has T-shaped and Z-shaped step-breaking channels. A large amount of organic acids formed by the thermal evolution of source rocks in the coal-bearing strata of the coastal plain facies of the Yacheng Formation (T80-T70) can be transported to the dense sandstone of the sand body of the Lingshui Formation (T70-T60) along the transport and accumulation channel system formed by the fault fractures in the northern fault zone. The main manifestation is that the clastic particles such as rock cuttings and feldspar are selectively eroded under the action of acidic fluids. Common feldspar dissolves in a honeycomb-like pattern or erodes along cleavage seams in a long strip shape. The edges and interiors of the cuttings are eroded to varying degrees, forming rich feldspar dissolution holes, intra-grain dissolution holes and mold holes [Figure 6(b) - Figure 6(e)]. The statistical results show that feldspar dissolution pores and mold pores are the main pore types in the third stage reservoirs of the Lingshui Formation in the study area, forming a pore type combination mainly composed of feldspar dissolution pores and mold pores [Figure 6(d)]. This paper comprehensively analyzes and concludes that the acidic fluids in the formation selectively dissolve feldspar substances and carbonate minerals, effectively increasing the pore volume, enhancing the throat connectivity, and significantly improving the physical properties of the reservoir sandstone. From the perspective of development scale, secondary pore development zones were formed in the three sections of the Lingshui Formation reservoir sandstone in the study area within the depth ranges of 3800m~3950m and 4100m~4400m, effectively improving the reservoir performance of tight sandstone reservoirs and providing enrichment sites and channels for oil and gas transport and accumulation as well as reservoir formation (Figure 12).

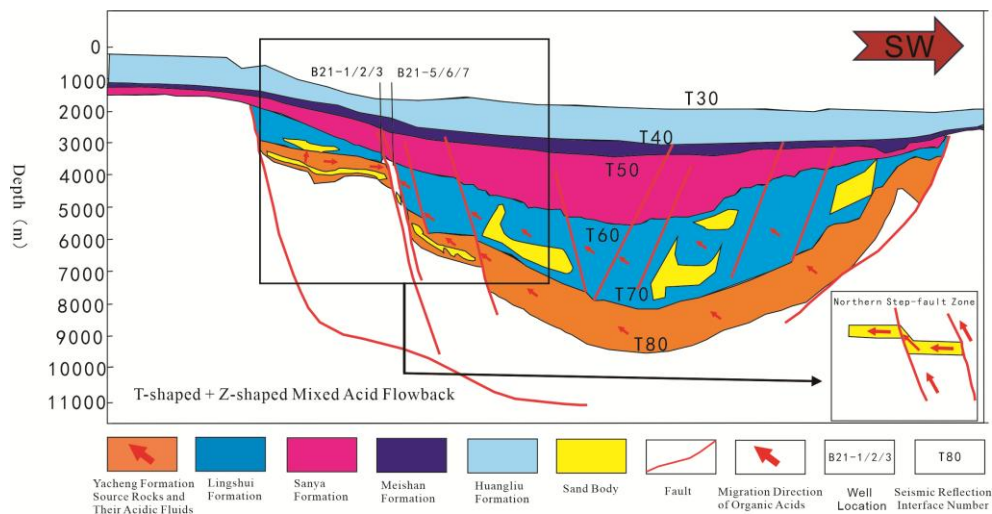


Figure 11. This is a figure. studies the conduction types and the formation mechanism of sweet spot reservoirs in the northern stage fault zone of the third section of the district Mausoleum.

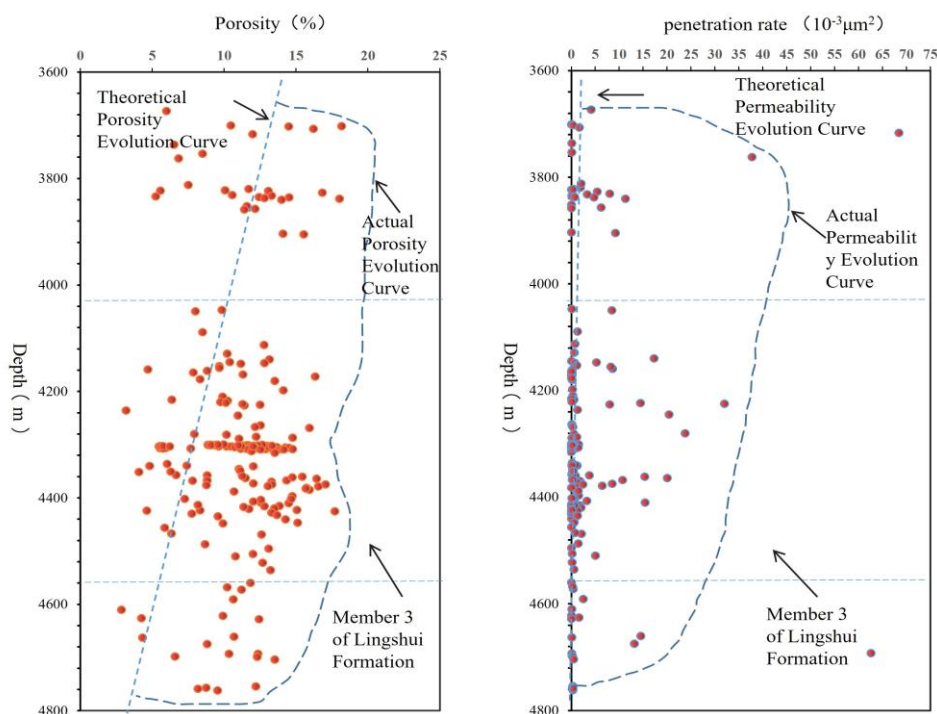


Figure 12. This is a figure. shows the pore infiltration development zone formed by the dissolution of the dense sandstone reservoir in the third section of the Lower Oligocene Ridge in the study area.

5.6. Analysis and Discussion on the Pore Development and Evolution Model of Tight Sandstone Sweet Spot Reservoirs

The three sandstone sections of the Lingshui Formation in the study area have undergone strong diagenetic transformation. The typical diagenetic processes include three main types: mechanical compaction, dissolution and cementation. However, there are obvious differences in the diagenetic evolution paths of feldspar quartz sandstone reservoirs, cuttings feldspar quartz sandstone reservoirs and feldspar cuttings quartz sandstone reservoirs, and their influences on the physical property evolution of the reservoirs are also different.

4.6.1. Feldspar quartz tight sandstone reservoir

The feldspar quartz sandstone in the study area is characterized by high quartz and feldspar content and low cuttings content. Compaction is mainly manifested as the sliding, rotation and compacting of rigid particles until they are in close contact or even undergo pressure dissolution. Under the extrusion of rigid particles, elongation deformation of plastic cuttings is observed. Compaction and solubilization significantly reduce the primary pores [Figure 6(d)]. Clastic sediments suffered from compaction and dehydration, volume reduction, and rapid shrinkage of primary pores during the early formation A period. The pore fillers are mainly clayey impurities, carbonate cements and autogenic clays. The native clay is mainly montmorillite-grade chlorite clay film (0.0%~0.3%, with an average of 0.01%). A small amount of calcite was cemented (0.0%~18.0%, with an average value of 0.28%), and the porosity was approximately 31.45%.

The strata were affected by rapid settlement. By the early rock formation B period, the feldspar quartz sandstone further underwent diagenetic transformation. Quartz particles further undergo rotation and rearrangement, and a small amount of plastic rock cuttings particles suffer slight elongation deformation. At this stage, the cementing material is mainly autogenic clay, with a small amount of siliceous cementing (0.0%~1.0%, with an average value of approximately 0.25%), and the porosity is about 18.55%.

In the A1 stage of Zhongchengyan, as the burial depth of the sediment increases, the solubility between the clastic particles enhances (pressure dissolution), resulting in some particles mainly

having concave-convex and linear contact. Secondly, a small amount of siliceous substances in the pore fluid are produced in the form of secondary enlarged edges. The intense compaction and deformation of the rock cuttings particles cause the reduction of the pores between the primary particles. During this period, the pore type was mainly residual intergranular pores, with a porosity of approximately 8.20%.

In the A2 stage of Zhongchengyan, acidic fluids formed from the thermal evolution of source rocks in the coastal plain coal-bearing strata of the Yacheng Formation selectively eroded feldspar and rock cuttings, resulting in pore combination types such as the remaining intergranular pores, feldspar dissolution pores and mold pores of the third section of the Lingshui Formation. With the development of dissolution, the average porosity of dissolution holes is approximately 7.16%. A small amount of cementites such as kaolinite (0.01~0.5%, with an average of 0.01%), illite (0.01~0.5%, with an average of 0.02%), and autogenic quartz (0.0%~1.5%, with an average of 0.35%) were produced and filled the intergranular pores. During this period, the pore types were mainly mold pores and feldspar dissolution pores. The porosity is approximately 14.98%.

During the B phase of Zhongchengyan, as the acidic environment gradually transformed into an alkaline one, the mutual transformation of clay minerals began. Such as kaolinite, chlorite, immorillonite mixed layer, montmorillonite and disordered immorillonite/immorillonite mixed layer clay undergoing illicization, etc. With the increase of stratum burial depth and temperature, mechanical compaction further leads to the reduction of intergranular pores in sandstone. At the same time, late iron calcite (0~25%, with an average of 1.86%) and iron dolomite (0~20%, with an average of 1.99%) and other materials unevenly fill the intergranular pores. The secondary cementation of quartz further developed. At this stage, the clay minerals are mainly late leaf-like chlorite and filamentous illite [Figure 2(i)]. The pore type of this period is mainly residual intergranular pores, with a porosity of approximately 10.92%.

4.6.2. Rock cuttings feldspar quartz tight sandstone reservoir

The quartz content of feldspar quartz sand in the rock cuttings ranges from 40.0% ~66.5%, with an average of 55.6%. The feldspar content ranged from 8.0%~18.5%, with an average of 12.8%, and the rock debris content ranged from 7.0%~12.0%, with an average of 9.2%. Due to the relatively high content of cuttings in feldspar quartz sandstone reservoirs, the deformation of plastic cuttings is more intense. Under the extrusion of rigid particles, the intense deformation of plastic cuttings is one of the important factors affecting pore evolution. The compaction of clastic sediments in the A stage of early rock formation is relatively weak, and the pore type is mainly residual intergranular pores. The average OP(initial Porosity) is approximately 40.0%. At this stage, the intergranular fillings are mainly early clay minerals, carbonate cements and argillaceous impurities, while the self-generated cements are mainly a small amount of early montmorillonite and chlorite (0.0%~0.5%, with an average of 0.05%), a small amount of early calcite (0.0%~33.0%, with an average of 0.35%), etc. The porosity is approximately 30.6%.

In the B stage of early rock formation, the plastic cuttings undergo slight deformation, resulting in a reduction of approximately 12.6% in intergranular pores. At this stage, the autogenous cementation mainly consists of autogenous chlorite, kaolinite and illite and other minerals (0.05%~0.8%, with an average of 0.12%), a small amount of siliceous substances (0.0%~1.5%, with an average of 0.38%), and the porosity is approximately 17.5%.

In the A1 stage of Zhongchengyan, under the action of mechanical compaction, rigid particles continue to squeeze plastic particles, causing the plastic rock cuttings to deform strongly and occupy the intergranular pores, thus forming a dense pore appearance. The porosity is approximately 7.81%.

By the middle stage of rock formation A2, the acidic fluid led to a relatively thorough dissolution of feldspar and rock cuttings, forming a pore combination type mainly consisting of feldspar dissolution pores and mold pores, as well as in-grain dissolution pores. The average porosity of the erosion holes is approximately 8.68%. The development of dissolution is accompanied by a large amount of kaolinite (0.0%~0.8%, with an average of 0.04%), chlorite (0.0%~1.3%, with an average of

0.07%), illite (0.0%~1.6%, with an average of 0.13%), and native quartz (0.4%~3.0%). The average value is 0.63% and other cementing substances are produced and fill the intergranular pores. The porosity is approximately 15.62%.

In the middle diagenesis stage B, under the alkaline diagenesis environment, the sandstone further densifies. In the late stage, iron calcite (0.0%~27%, with an average of 2.08%) and iron dolomite (0.0%~10%, with an average of 2.01%) and other materials unevenly fill the intergranular pores. At this stage, the clay minerals are mainly late chlorite and illite, with a porosity of approximately 11.48%.

4.6.3. Feldspar quartzite tight sandstone reservoir

The quartz content of feldspar quartzite sand ranges from 46.0%~67.0%, with an average of 56.6%. The feldspar content ranged from 8.5%~12.0%, with an average of 9.3%, and the cuttings content ranged from 9.0%~13.0%, with an average of 10.1%. High-plasticity feldspar quartzite sandstone still develops a certain amount of calcite cementation (0.0%~22%, with an average of 1.83%) and autogenic clay (montmorillite, chlorite clay film) (0.0%~0.5%, with an average of 0.1%) in the early diagenetic stage. Compared with other types of rock facies reservoirs, the early calcite cementation content is relatively high. However, the cementation content of the early autogenous clay was relatively high. The porosity is approximately 28.5%.

In the early formation A stage, under the heavy load of the overlying strata, the loose sediment was continuously compacted, resulting in a sharp reduction in porosity. At this stage, intergranular pores are predominant. As the rocks are closely compacted, plastic volcanic cuttings start to deform. The porosity is approximately 19.5%.

In the B stage of early rock formation, the strong compaction and the compression of rigid quartz particles led to relatively strong plastic deformation of volcanic rock cuttings, which in turn caused a sharp reduction in the intergranular pores. The porosity is approximately 15.8%.

By the Middle diagenetic stage A1, volcanic cuttings underwent intense plastic deformation. The deformation of cuttings led to the extensive filling of the residual intergranular pores, forming a dense reservoir physical property background. During this period, the residual intergranular porosity was approximately 11.67%.

In the A2 stage of Zhongchengyan, the acidic fluid in the pore fluid slightly eroded the rock cuttings particles, forming a pore combination type mainly composed of feldspar dissolution pores and mold pores, as well as in-grain dissolution pores. The average porosity of the dissolution pores is approximately 5.77%. Illite (0.0%~0.5%, with an average of 0.11%), autogenic quartz (0.3%~1.5%, with an average of 0.65%), and other cementing materials are produced and fill the intergranular pores, with a porosity of approximately 16.68%.

In the B stage of rock formation, mechanical compaction led to intense deformation of plastic cuttings, further reducing the intergranular pores. Secondly, in the late stage, iron calcite (0.0%~25%, with an average of 5.23%) and iron dolomite (0.0%~5.5%, with an average of 1.01%) unevenly filled the intergranular pores, resulting in further densification of the sandstone. At this stage, the autogenic clay minerals are mainly late chlorite and illite. Notably, with the intensification of plastic deformation of volcanic cuttings, the secondary increase of quartz in the middle igneous stage and the autogenic cementation of clay minerals are significantly inhibited, with a porosity of approximately 10.21% (Figure 13).

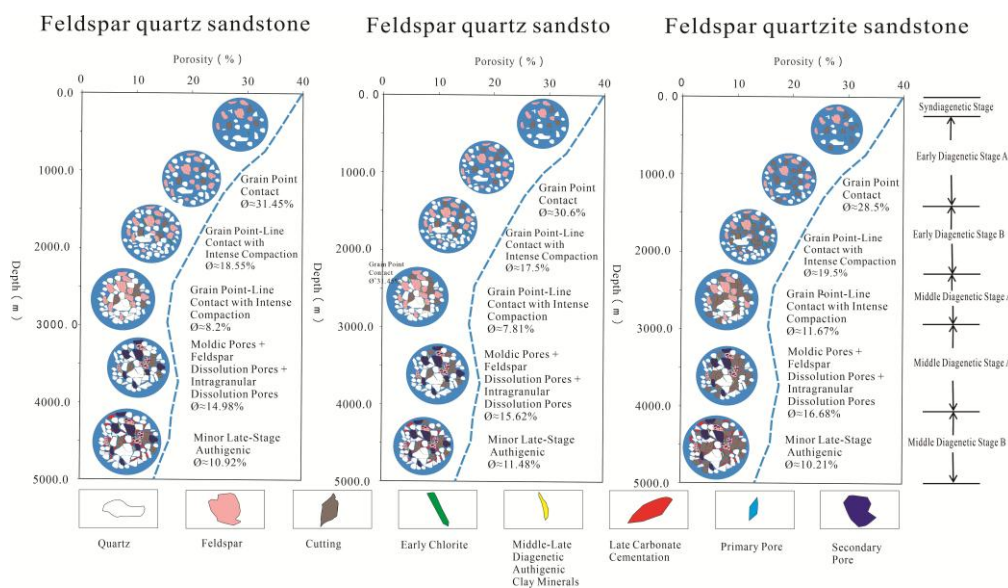


Figure 13. This is a figure. shows the diagenesis and pore development and evolution patterns of the tight sandstone reservoirs in the third section of the study area.

6. Conclusions

(1) In the deep water area of the Northern Slope of the Baodao Depression, the three tight sandstone reservoirs of the middle and deep Oligocene Lingshui Formation mainly develop feldspar quartz sandstone, feldspar quartz sandstone and feldspar feldspar quartz sandstone. The pore types are mainly feldspar dissolution pores, mold pores and intergranular pores. Among them, the feldspar quartz sandstone and feldspar quartz sandstone have relatively good reservoir physical properties and belong to sweet spot reservoirs conducive to oil and gas occurrence.

(2) High content of quartz and feldspar and relatively low content of cuttings are one of the main controlling conditions for the formation of sweet spot reservoirs in middle and deep tight sandstone. Grain size has a good positive correlation with the reservoir physical properties of the reservoir, and diagenesis is the key to the development and evolution of tight sandstone sweet spot reservoirs. Compaction led to a loss of 22.0%~28.0% of the porosity of sandstone, with an average of 24.0%. Due to the dissolution effect, dissolution pores are formed, which greatly increases its porosity and permeability.

(3) Due to the thermal evolution of hydrocarbon generation in the coastal plain facies of the Yacheng Formation of the Lower Oligocene in the study area, a large amount of organic acids were produced, which led to the dissolution of feldspar and the formation of a large number of feldspar dissolution pores and mold pores. Therefore, secondary pore development zones were formed in the depth sections of 3800m~3950m and 4100m~4400m in the three tight sandstone sections of the Lingshui Formation. It constitutes the sweet spot zone in the tight sandstone reservoir. Therefore, dissolution is the key to the formation of sweet spot reservoirs in tight sandstone.

(4) The pore development and evolution model of tight sandstone indicates that the differential diagenetic evolution is the main reason for the distinct reservoir physical properties of the three tight sandstone reservoirs in the Lingshui Formation. In the tight reservoirs of feldspar quartz sandstone and cuttings, the high content of feldspar particles and the relatively low content of cuttings, along with the extensive dissolution of feldspar in the middle and late stages, are the key factors for the improvement of the reservoir physical properties of this type of tight sandstone reservoir. In feldspar quartz-sandstone tight reservoirs, the content of rock cuttings is high. Due to the strong deformation and weak dissolution modification of plastic rock cuttings, it often leads to further densification of the reservoir, which is not conducive to the formation of sweet spot reservoirs.

References

1. Du Guichao, Liu Junfeng, Guo Ruiliang, et al. Development Characteristics and Influencing Factors of high-quality Reservoirs in Section 8 of the southeastern Ordos Basin [J/OL]. *Natural Gas Geoscience*.<https://link.cnki.net/urlid/62.1177.TE.20240826.1820.002>
2. Sun Longde, Zou Caineng, Zhu Rukai, et al. Analysis of Formation, Distribution and Potential of Deep Oil and Gas in China [J]. *Petroleum Exploration and Development*,2013,40(6):641-649.
3. Yang Hua, Li Shixiang, Liu Xianyang. Characteristics and resource potential of tight oil and shale oil in the Ordos Basin [J]. *Acta Petrolei Sinica*,2013,34(1):1-11.
4. Zou Caineng, Zhu Rukai, Bai Bin, et al. Connotation, characteristics, potential and challenges of tight oil and shale oil [J]. *Bulletin of Mineralogy, Petrology and Geochemistry*,2015,34(1):3-17,1-2.
5. Yang Xiulei, Wu Zhenyun, Yin Hongwei, et al. Experimental Simulation of the Influence of Basement Slope Folds on the Formation and Evolution of Salt Overlying fold Impulse Structures: A Case Study of the Miscantak Anticline in the Western Section of Kuqa Depression [J]. *Tectonics and Metallogeny*, 2020,49(1):57-69.
6. Liu Li, Zhang Kaixun, Yu Gang, et al. Central Asia main salt basin, the hydrocarbon accumulation characteristics and main control factors of enrichment of [J]. *Geological oil experiment*, 2025,47 (2) : 336-346. The DOI: 10.11781 / sysydz2025020336.
7. Kirschning. A, AltwickerC, DragerG, et al. PASSflow Syntheses Using Functionalized Monolithic Polymer/Glass Composites in Flow-Through Microreactors Part of these studies were supported by the Fonds der Chemischen Industrie and the European Community (EC project number HPRI-CT-1999-00085) for which[J].*Angewandte Chemie*, 2010 (8) : no - no. DOI: 10.1002 / chin. 200208062.
8. Plint.A.G.Facies,environments and sedimentary cycles in the Middle Eocene, Bracklesham Formation of the Hampshire Basin:evidence for global sea-level changes? [J]. *Journal of Sedimentology*, 1983, 30 (5), DOI: 10.1111/1365-3091.1983. J. tb00699. X.
9. Smith M G ,Bustin R M.Late Devonian and Early Mississippian Bakken and Exshaw Black Shale Source Rocks, Western Canada Sedimentary Basin:A Sequence Stratigraphic Interpretation[J].*Aapg Bulletin*, 2000,84 (7). DOI: 10.1306 / A9673B76 c1865d d7-1738-11-8645000102.
10. S,O,Egenhoff,et al.Traces In the Dark--Sedimentary Processes and Facies Gradients In the Upper Shale Member of the Upper Devonian-Lower Mississippian Bakken Formation, Williston Basin, North Dakota, U.S.A [J]. *Journal of Sedimentary Research*, 2013 turned (9) : 803-824. The DOI: 10.2110 / JSR. 2013.60.
11. Meissner.Petroleum Geology of the Bakken Formation Williston Basin,North Dakota and Montana [J]. [2025-09-25]. DOI: 10.1306 / m35439c9.
12. Hlidek B T,Rieb B A.Fracture Stimulation Treatment Best Practices in the Bakken Oil Shale [J]. [2025-09-25]. DOI: 10.2118/140252 - MS.
13. Pollastro R M.GEOLOGIC MODEL FOR ASSESSMENT OF TECHNICALLY RECOVERABLE OIL IN THE DEVONIAN-MISSISSIPPIAN BAKKEN FORMATION, WILLISTON BASIN,U.S.A[J].2012.
14. Downey R,Venepalli K.Application of Two Novel Enhanced Oil Recovery Processes in the Bakken Shale[J].*SPE-Society of Petroleum Engineer*,2023,000(3-23WRM):11.DOI:10.2118/212984-MS.
15. Lima R D ,Ros L F D.The role of depositional setting and diagenesis on the reservoir quality of Devonian sandstones from the Solimes Basin,Brazilian Amazonia[J].*Marine and Petroleum Geology*, 2002, 12 (9) : 1047-1071. The DOI: 10.1016 / S0264-8172 00002-3 (03).
16. Rezende M F,Pope M C .Importance of depositional texture in pore characterization of subsalt microbialite carbonates, offshore Brazil[J].*Geological Society London Special Publications*,2015,418(1):193-207.DOI:10.1144/SP418.2.
17. Zeitoum N,Vidal A C,Ruidiaz E M.Petrographical and petrophysical characterization of pre-salt Aptian carbonate Reservoirs from the Santos Basin, Brazil [J]. *Journal of Petroleum team*, 2024, 30 (1) : 56-75. The DOI: 10.1144 / petgeo2023-045.
18. Santos G O R D,Ribeiro G S D S,Ventura L.Multi-Technique Characterization of Carbonate Lithotypes and Evaluation of the Impact of Fine Grains on Barra Velha Formation Reservoirs,Sepia Field, Santos

- Basin[J].SPWLA-Society of Petrophysicists and Well Log Analysts, 2024000 (4 - SPWLA24) : 21. DOI: 10.30632 / SPWLA - 2024-0079.
19. Moreira J,Garcia L,Ceia M,et al.Comparison between methodologies of cementation exponent in carbonate reservoir of Santos Basin, Brazil [J]. Journal of 84th EAGE Annual Conference & Exhibition, 2023. The DOI: 10.3997/2214-4609.202310995.
 20. Gu C,Xiang M,Li M,et al.The Casing Collapse Mechanism in Salt Formations in Deepwater Fields in Brazil [J]. The Processes, 2025, 13, DOI: 10.3390 / pr13020301.
 21. Gao W,Zhang Q,Zhao J,et al.Transitional shale reservoir quality evaluation based on Random Forest algorithm—a case study of the Shanxi Formation,eastern Ordos Basin,China[J].Earth Science Informatics, 2025, 19 (1) : 1-20. DOI: 10.1007 / s12145-024-01515 - z.
 22. BAIYun-lai,ZHAO-Yingcheng,Long M A ,et al.Geological Characteristics and Resource potentials of Oil Shale in Ordos Basin,Center China[C]//World energy conference.2010.
 23. Liu Z,Yan Q.Can farmland ownership confirmation promote farmers' adoption of conservation tillage techniques:empirical evidence from the Yellow River Basin in China[J].FRONTIERS IN SUSTAINABLE FOOD SYSTEMS, 2024, 8 (000) DOI: 10.3389 / fsufs. 2024.1537024.
 24. Andrea,Miccoli,Giorgia,et al.Beneficial bacteria affect Danio rerio development by the modulation of maternal factors involved in autophagic,apoptotic and dorsalizing processes.[J].Cellular physiology and biochemistry : the international journal of experimental cellular physiology, biochemistry, and pharmacology, 2015. The DOI: 10.1159/000373983.
 25. Yang C,Zhang J,Tang X.Microscopic pore types and its impact on the storage and permeability of continental shale gas,Ordos Basin[J].Earth Science Frontiers,2013,20(4):240-250.
 26. Deng Xiaoliang, Wang Ziling, You Li, et al. The Development characteristics of Braided river deltas under the control of the Fault-stage Zone Geomorphology in the Qiongdongnan Basin: A Case Study of the Third Section of the Oligocene Lingshui Formation on the Northern Slope of the Baodao Depression [J] Marine Petroleum Geology, 2020,30(1):30-40.
 27. You Li, Li Wei, Li CAI, et al. Main controlling factors of physical properties of deep-buried reservoirs in Baodao Area, Qiongdongnan Basin [J] Special Oil and Gas Reservoirs, 2014,21 (3):37-131.
 28. Shan Xiang, Guo Huajun, Chen Xiguang, et al. The densification formation of low-permeability tight sandstone reservoirs: A Case Study of the Lower Jurassic Badaowan Formation in the Mobei-Mosuowan Uplift of the Junggar Basin [J]. Xinjiang Petroleum Geology,2021,42(1):29-37.
 29. Xu Changgui, You Li. Characteristics of the Northern Slope Transition Zone of Songnan-Baodao Depression in Qiongdongnan Basin and Its control over Large and Medium-sized Gas Fields [J] Petroleum exploration and development, 2022,49 (6) : 1061-1072. The DOI: 10.11698 / PED. 20220102.
 30. Guo Shusheng, Liao Gaolong, Liang Hao, et al. Major Breakthrough and Significance in Deepwater Natural Gas Exploration of Well BD21 in Qiongdongnan Basin [J] China Petroleum Exploration,2021,26(5):49-59.
 31. Zhu Peiyuan, Yuan Qingtao, You Li, et al. Island in the basin in the southeast area lingshui group reservoir characteristics and distribution of favorable reservoir [J]. Journal of natural gas technology and economy, 2020, 14 (1) : 6. DOI: CNKI: SUN: TRJJ. 0.2020-01-004.
 32. Zhong Jia, You Li, Zhang Yingchao, et al. Diagenesis and pore evolution of canyon waterway reservoirs in Huangliu Formation, Ledong-Lingshui Depression, Qiongdongnan Basin [J] Gas earth science, 2018, 29 (5) : 11. DOI: 10.11764 / j.i SSN. 1672-1926.2018.01.002.
 33. Zheng Lei, Yan Zhuoyu, Li Donglin, et al. Comparative Analysis of Reservoir Physical Properties in Lingshui Sag, Qiongdongnan Basin [J]. Petrochemical Technology,2021(8).135-148.
 34. Gan Jun, Zhang Yazhen, Lin Lu, et al. Main controlling factors and accumulation models of differential natural gas accumulation in Baodao Sag, Qiongdongnan Basin [J]. Earth Science, 2023, 48(2):439-450.
 35. Tan Jiancai, Fan Caiwei, Ren Keying, et al. The tectonic transformation zone in the northern Qiongdongnan Basin and its significance in oil and gas geology [J]. Oil Geology and Recovery Efficiency, 2014, 21 (2) : 62-65
 36. Yang Xibing, Fu Heng, He Xiaohu, et al. The neogenic sedimentary system and its structure-sedimentary evolution in the southern uplift zone of the Qiongdongnan Basin [J]. Sedimentary and Tethian geology, 2019,39 (3) : 1-10

37. Zhou Jie, Yang Xibing, Yang Jinhai, et al. Tectonic-sedimentary evolution characteristics and Natural gas accumulation of the Paleogene in the Songnan Low Uplift, Qiongdongnan Basin [J]. Earth Science, 2019,44 (8) : 2704-2716.
38. Jing Taotao, Li Wenhao, Dong Wei, et al. Coupling Relationship between Reservoir densification process and Oil and Gas Charging in the Ahe Formation in the Dibei area of Kuqa Depression [J] Modern geology, 2025, 33 (4) : 6, 1156-1168. The DOI: 10.19657 / j.g eoscience. 1000-8527.2024.072.
39. Zhuang Songsheng, Zuo Yanchun, Li Qiong. North jiangsu dainan group 2 Duan Chengyan qintong sag effect and secondary porosity prediction [J]. Journal of mineral rocks, 2025, 17 (4) : 64. DOI: 10.19719 / j.carol carroll nki. 1001-6872.1998.04.011.
40. Li Xiwei, Jiang Shu, Shi Yuanpeng, et al. Analysis of Characteristics and Reservoir Control Factors of Deep Clastic Rock

Disclaimer/Publisher's Note: The statements, opinions and data contained in all publications are solely those of the individual author(s) and contributor(s) and not of MDPI and/or the editor(s). MDPI and/or the editor(s) disclaim responsibility for any injury to people or property resulting from any ideas, methods, instructions or products referred to in the content.